

Variability in surface energy flux partitioning during Washita '92: Resulting effects on Penman–Monteith and Priestley–Taylor parameters

William P. Kustas^{a,*}, David I. Stannard^b, K. Jerry Allwine^c

^a *Agricultural Research Service, US Department of Agriculture, Beltsville, MD 20705, USA*

^b *Water Resources Division, US Geological Survey, Denver, CO, USA*

^c *Atmospheric Sciences Department, Pacific Northwest Laboratories, Richland, WA, USA*

Received 6 February 1995; accepted 8 December 1995

Abstract

During the Washita '92 field experiment, the local surface energy balance was evaluated at four locations in the USDA–ARS Little Washita River Watershed near Chickasha, OK, using the Bowen ratio–energy balance (BREB) approach. For any given day, differences in the partitioning of the available energy appeared to be mostly a function of the type of vegetation at the site, while the actual magnitude of the fluxes was mostly affected by cloud cover. The soil surface was initially wet, and gradually dried during the field experiment. However, there was not a corresponding decrease in the evaporative fraction, which would have indicated a decreasing contribution of soil evaporation to the total latent heat flux. Ground weather data indicated a large shift in the direction and magnitude of the surface winds, and a significant increase in air temperature and vapor pressure deficit. During this period, the evaporative fraction actually increased at two of the four sites. The response of the different sites to the changing near-surface atmospheric conditions was studied in more detail by evaluating the canopy resistance (r_c) to evaporation using the Penman–Monteith equation and the Priestley–Taylor parameter (α). Midday averages of r_c and (α) tended to decrease (increase) with increasing vapor pressure deficit for two of the sites while such a trend was not evident for the other two sites. Estimates of stomatal resistances indicated that significant plant physiological differences existed between the sites containing weedy vegetation versus the grasses at the pasture/rangeland sites. Even though soil moisture conditions were relatively wet, α was less than 1 at all sites and there was no trend in α as a function of surface soil moisture conditions. These findings suggest that vegetation types

* Corresponding author.

in mixed agricultural/rangeland ecosystems can have significantly different responses to similar atmospheric forcing conditions.

1. Introduction

One of the major goals of recent large scale interdisciplinary field experiments is to improve the parameterization of land surface–atmosphere exchange processes. This will lead to improvements in atmospheric model simulations of the transport of latent (λE) and sensible (H) heat fluxes over different landscapes, and ultimately result in better weather forecasting and predictions (e.g. Beljaars et al., 1993). However, there is still debate as to the complexity required in atmospheric models to compute land surface fluxes (Avissar, 1993). The concept of scale decoupling developed by Jarvis and McNaughton (1986) and McNaughton and Jarvis (1991) indicates that including complex relations found at the leaf scale may not be necessary at the field (or canopy) and larger scales. This theory has been supported by observations (e.g. Avissar, 1993; Baldocchi, 1989) and helps to explain why Penman–Monteith and Priestley–Taylor evaporation equations continue to be applied, especially over short vegetation (e.g. Crago and Brutsaert, 1992; Stewart and Verma, 1992).

In this paper, the spatial and temporal variation in the surface energy balance estimates at four locations within the Little Washita River Watershed, Oklahoma will be investigated. The data were collected during the Washita '92 field experiment (Jackson et al., 1993a). The partitioning of net radiation (R_n) and soil heat flux (G) or the available energy into evaporation, expressed as the evaporative fraction ($EF = \lambda E / (R_n - G)$), was evaluated at each site. Penman–Monteith (Monteith, 1973) and the Priestley–Taylor (Priestley and Taylor, 1972) equations were used to estimate canopy resistance (r_c) and the α parameter at each site. With estimates of leaf area index (LAI), representative values of stomatal resistance (r_s) for each site were computed and compared. Comparison of r_s -values among the sites indicated that differences in plant physiology was probably the main factor causing the site-to-site variability in EF, and associated variation in r_c and α .

2. Theory

The canopy resistance, r_c , was computed by rearranging the Penman–Monteith equation to yield

$$r_c = \frac{\left[\Delta(R_n - G) + \frac{\rho c_p (e_a^* - e_a)}{r_{av}} - \Delta \lambda E \right] r_{av}}{\gamma \lambda E} - r_{av} \quad (1)$$

where Δ is the slope of the saturation water vapor pressure curve at air temperature T_a , e_a^* is the saturation vapor pressure at the reference level where T_a is measured (z_T), e_a is the actual vapor pressure, ρ is the air density, c_p is the heat capacity of air, γ is the

psychrometric constant, r_{av} is the aerodynamic resistance to water vapor transfer, R_n is the net radiation, G is the soil heat flux and λE is the latent heat flux. The value of r_{av} was estimated using Monin–Obukhov surface layer similarity theory yielding

$$r_{av} = \frac{\left[\frac{\ln(z_u - d_o)}{z_{om}} - \psi_m \right] \left[\frac{\ln(z_T - d_o)}{z_{ov}} - \psi_v \right]}{k^2 u} \quad (2)$$

where d_o and z_{om} are the displacement height and roughness length for momentum, ψ_m and ψ_v are the Monin–Obukhov surface layer stability correction functions for momentum and water vapor, respectively (see Brutsaert, 1982), u is the wind speed measured at height z_u , k is the von Kármán's constant (0.4), and z_{ov} is the roughness length for water vapor. The value of z_{ov} for grass type vegetation was taken as a fraction of z_{om} , namely $z_{ov} = z_{om}/7$ (Brutsaert, 1982).

Observations (e.g. Baldocchi, 1989; Baldocchi et al., 1991) and theoretical work by Finnigan and Raupach (1987) indicate that r_c computed by Eq. (1) can differ significantly from leaf-scale measurements or multi-layer models integrated to the canopy scale. However, Kim and Verma (1991) found good agreement in computing r_c scaling up from leaf to the canopy level with estimates using Eq. (1) for a grassland prairie site.

To gain a better measure of plant physiological differences between sites, representative values of the stomatal resistance (r_s) were computed. These values were determined by assuming that r_c is the equivalent resistance of all the individual stomates in a canopy, taken in parallel. Thus the relationship between r_s (where the value of r_s is defined as being representative of all individual stomates) and r_c is given by the following expression (Shuttleworth, 1976):

$$r_s = \text{LAI } r_c \quad (3)$$

The value of the Priestley–Taylor parameter α is computed by

$$\alpha = \frac{\lambda E (\Delta + \gamma)}{\Delta (R_n - G)} \quad (4)$$

A value for α of 1.26 has been adopted for most wet surfaces (Brutsaert, 1982); however Flint and Childs (1991) report α values, computed from a collection of studies over various landscapes, that range from nearly 1.6 to 0.7. The variation in α reported from experimental data has been related to canopy resistance from model simulations of atmospheric boundary layer development (de Bruin, 1983; McNaughton and Spriggs, 1989). Other efforts have explored the relationship between α and leaf area index (LAI) and cumulative soil evaporation (Stannard, 1993) and surface soil moisture (e.g., Barton, 1979; Davies and Allen, 1973; Crago and Brutsaert, 1992).

3. The experiment

The Washita '92 experiment took place in the Little Washita River Basin (34.8° N; 98.2° W) near Chickasha, OK, from June 8–19, 1992. The basin is approximately 610

km² in area and drains into the Washita River. The terrain is a mildly hilly mixture of rangeland, pasture and cropland with smaller areas of forests, urban/highways, oil waste land, quarries and reservoirs (Allen and Naney, 1991). The Washita '92 experiment was a cooperative effort between USDA, NASA, USGS and several other government agencies and universities. The main objective of the experiment was to evaluate the utility of remotely sensed data for quantifying surface energy and hydrologic fluxes from local to basin scales. The testing and verification of several new remote sensing devices and the development of data bases for target–sensor interaction algorithms were other specific goals of the project. The types of ground-, aircraft- and satellite-based remote sensing data, and hydrologic and meteorological data are summarized in Jackson et al. (1993a).

The intensive data collection campaign covered the period from June 10 through June 18, 1992, or Day of Year (DOY) 162–170. The field campaign followed a period of intense rain storms which occurred over several weeks, ending on June 9, DOY 161. At the start of the observations, the soil surface across the basin was wet and standing water was present in many of the agricultural fields. No rain events occurred during the experimental period, resulting in gradual drying of the near-surface soil.

4. Methods

To evaluate the energy balance over non-forested land surfaces and under non-advective conditions requires the determination of four flux components, which are related by

$$R_n - G - H - \lambda E = 0 \quad (5)$$

Under daytime convective conditions, typically R_n , G , H and λE are positive. At the four sites, R_n and G were measured using thermopile devices, and the turbulent fluxes H and λE were measured using the BREB (Bowen-ratio energy balance) method.

The BREB method is based on the assumption that the eddy diffusivities for H and λE in the atmospheric surface layer are equal (Bowen, 1926). The Bowen ratio, β , which is the ratio of H to λE , can then be measured as:

$$\beta = \gamma \frac{\Delta T}{\Delta e} \quad (6)$$

where γ is the psychrometric constant, ΔT is the temperature difference between two elevations above a plant canopy, and Δe is the vapor-pressure difference between the same two elevations.

Combining Eq. (5) with the definition of β leads to:

$$\lambda E = \frac{R_n - G}{1 + \beta} \quad (7)$$

H is then calculated from Eq. (5). Calculated values of λE and H are dependent on measurements of R_n , G , ΔT and Δe , and on the validity of the advection and eddy-diffusivity assumptions. Net radiation, R_n , was measured using thermopile type, shielded net radiometers. Soil heat flux, G , was measured using the combination method

(Tanner, 1960), which involves burying heat flux plates at a depth of several centimeters, and measuring the change in soil temperature above the plates. The BREB method has been tested by numerous investigators and it is thought to have an uncertainty of 10% for λE under ideal conditions (Sinclair et al., 1975). For heterogeneous surfaces, however, the uncertainty probably increases to 20% (Nie et al., 1992).

5. Site and measurement description

The four surface flux sites were located in the western, north-central, south-central and northwestern portions of the watershed. In Fig. 1, the approximate location of the four stations along with main drainages and highways are illustrated. In addition to the energy flux data, various standard weather data (air temperature, humidity, wind speed and direction, barometric pressure), and supplementary data (soil moisture, soil temperature, solar radiation, photosynthetically active radiation) were collected routinely (Stannard et al., 1993).

Soil cores were obtained daily using a Soilmoisture Equipment Corp. 200-A soil core sampler. These cores extended from the surface to a 6-cm depth, and were used to determine bulk density and moisture content. Nine gravimetric soil moisture samples were also collected on a square grid basis (10 m apart) each day using a specifically

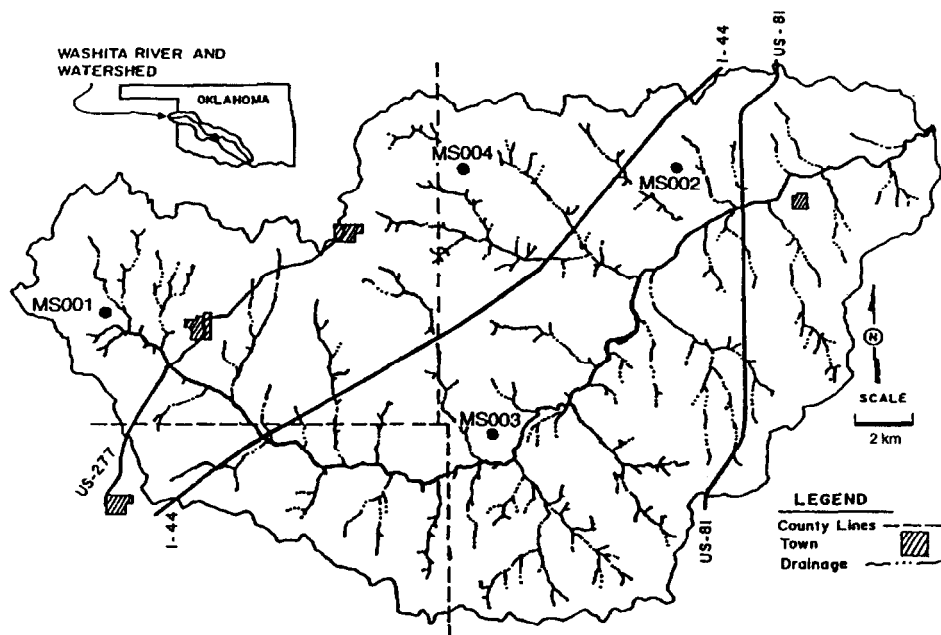


Fig. 1. Boundary of the Little Washita Watershed located within the Washita Basin in Oklahoma along with its drainage network. Major towns and roads are indicated as well as the approximate location of the four flux stations, MS001, MS002, MS003 and MS004. Adapted from Allen and Naney (1991).

Table 1

Near-surface soil texture for the fields containing the four flux stations

Flux Station	Soil Texture (% by weight)		
	Sand	Silt	Clay
MS001	38	44	18
MS002	45	45	10
MS003	88	9	3
MS004	84	12	4

designed tool that extracts a 5 cm cube of soil. The bulk density for each site was measured using a volumetric displacement procedure with a specifically designed bulk density ring having a hook gage and securing bolts (Jackson et al., 1993c). Soil texture for the upper 5 cm was determined at a number of sites in the watershed, including the four flux stations. Percentages of sand, silt and clay for each site, are listed in Table 1.

During the field campaign, the soil moisture profile was also monitored at a number of locations in the watershed, including the four surface flux sites (Heathman, 1993). The moisture profiles were obtained by a Resonant Frequency Capacitance (RFC) probe, a recently developed instrument with technology based upon the use of soil dielectric properties to measure water content (Dean et al., 1987; Bell et al., 1987). Measurements were taken at 15 cm intervals starting at a depth of approximately 7.5 cm down to a depth of nearly 120 cm. Although the method requires calibration with field data for accurate determination of soil water content, preliminary comparisons with soil core data by Heathman (1993) indicate the technique can give reliable results.

At each site, plant biophysical data were collected, including wet and dry biomass and for some sites, LAI (Williams, 1993). The procedure was to clip and weigh all vegetation within a 1 m² area. A representative sample was separated into leaves and stems; LAI was determined and fresh and dry weight of the subsample was also measured. The LAI and dry weight biomass of the clipped area were then calculated using the subsample data. In addition, a qualitative description was given for each site identifying the dominant vegetation species. In Table 2 a listing of vegetation type, wet and dry biomass and measured and estimated LAI; LAI was measured for MS002 and MS003. Since the vegetation structure at MS004 was similar to MS002, a value of LAI was estimated by multiplying the ratio of wet biomass of MS004 and MS002 by the LAI measured at MS002. For MS001, the structure of the weedy vegetation was significantly different from the vegetation at MS003. Therefore, LAI was estimated using an exponential relationship with fractional vegetation cover described by Choudhury et al. (1994) (see Fig. 11 in Choudhury et al., 1994).

5.1. Measurements at MS001

MS001 was located in a winter-wheat field that had been partially grazed and then allowed to revegetate. A single species of weed appeared to dominate (mustard, *Sinapis arvensis* L.), and was interspersed with dead wheat plants and common ragweed (*Ambrosia artemisiifolia* L.). Total percent cover was estimated to be around 50% with

Table 2
Vegetation information for the four flux stations

Station	Description (dominant species)	Wet biomass (kg m ⁻²)	Dry biomass (kg m ⁻²)	LAI (–)
MS001	Weeds, 50% Cover (Mustard, <i>Sinapis arvensis</i> L.)	0.582	0.224	1 ^a
MS002	Pasture/rangeland (Big bluestem, <i>Andropogon gerardii</i> , Vitman)	0.951	0.430	2.3
MS003	Weedy pasture (Mixture of grasses and forbs ^b)	0.561	0.194	0.86
MS004	Pasture/rangeland (Weeping lovegrass, <i>Eragrostis barrelieri</i> , Daveau.)	0.653	0.413	1.6 ^a

^a Estimated using biomass data or exponential relationship with fractional cover (see text).

^b Mixture of grasses and forbs that include: Queen-Annes-Lace *Daucus carota* L., Plantago *Plantago lanceolata* L., Thistle *Cirsium vulgare* (Savi) Tenore, Curly dock *Rumex crispus* L., Bermudagrass *Cynodon dactylon* (L.) Pers., Broomsedge *Anthropogon virginicus* L., Sunflower *Helianthus* sp. L.

average canopy height of about 0.50 m. The instruments were located approximately 50 m east of a north-south gravel road with a 3 m border of sorghum along the shoulder about 1 to 2 m in height, and about 130 m north of an area of standing water roughly 40 m in diameter. Using a fetch to height ratio of 50:1 for the BREB method (Heilman et al., 1989; M. Weseley, personal communication, 1994) adequate fetch existed for winds from the north, south and east with marginal fetch from the west (road).

Bowen-ratio, weather, and supplementary data were collected at MS001 from DOY 163 to DOY 171. Sensors and deployment heights and depths are listed in Table 3. R_n was measured using a REBS (Radiation Energy Balance Systems¹) Q6 net radiometer. G was measured using a combination method. Three Peltier-cooler soil-heat-flux plates (Weaver and Campbell, 1985) were buried at 5 cm to measure G_d , the flux at depth. Three 4-junction averaging thermocouple probes were used to measure the change in temperature of the soil between the surface and the 5-cm depth. The heat-storage flux, ΔST , in the 5-cm thick layer is:

$$\Delta ST = \Delta T_s \cdot C \cdot D / t \quad (8)$$

where ΔT_s is the change in mean soil temperature during the measurement period, C is the volumetric heat capacity of the soil, D is the depth of the plate, and t is the length of the measurement period. The soil-heat flux, G , is the sum of G_d and ΔST . The value of C was determined from estimates of bulk density and soil moisture.

Air-temperature and vapor-pressure differences were measured using a psychrometer exchange mechanism (Stannard, 1985). Two WVU-7 psychrometers, made by Delta-T Devices, were deployed above the plant canopy, separated vertically by 1 m. The psychrometers were scanned for 10 min, exchanged, and then were idle for 5 min, to equilibrate to the new temperatures. Measurements from two of these 15-min cycles

¹ Any use of trade, product, or firm names is for descriptive purposes only and does not imply endorsement by the US Government.

Table 3

Sensor deployment at MS001

Variable	Sensor make and model	Sensor height or depth (m)
Net radiation	REBS Q6	1.38
Deep soil-heat flux	Modified Peltier coolers (Weaver and Campbell, 1985)	– 0.05
Heat-storage flux	Thermocouples	– 0.006, – 0.019, – 0.031, – 0.044
Air-temperature difference	Delta-T WVU-7	0.84, 1.84
Vapor-pressure difference	Delta-T WVU-7	0.84, 1.84
Air temperature	Campbell Scientific HMP35C	1.55
Relative humidity	Campbell Scientific HMP35C	1.55
Wind speed	R.M. Young 03001-5	1.87
Wind direction	R.M. Young 03001-5	1.87
Solar radiation	Licor LI-200S	1.51
Photosynthetically active radiation	Licor LI-190S	1.51

were averaged to produce a 30-min Bowen ratio that was unaffected by sensor bias. All sensors used in the Bowen-ratio calculations were scanned every 5 s, and 15-min or 30-min means were recorded on a Campbell Scientific 21X data logger.

Air temperature and humidity were measured using a Campbell Scientific HMP35C probe. Wind speed and direction were measured using an R.M. Young 03001-5 wind sentry. Solar radiation and photosynthetically active radiation (PAR) were measured using a Licor LI-200S pyranometer and a Licor LI-190S quantum sensor, respectively. These sensors were scanned every 5 s, and average values were recorded on the 21X logger every 30 min. Average temperature in the top 5 cm of soil (used to calculate ΔST) was measured and recorded once every 30 min.

5.2. Measurements at MS002

MS002 was located in native pasture, densely vegetated with grasses, predominately big blue stem (*Andropogon gerardii* Vitman.), and some forbs. The canopy cover was nearly 100% with average vegetation height of around 0.6 m. The field was bordered on the north and south by wooded creeks, flowing west to east, about 200 m apart. The stands of trees were about 10 m high and about 20 m wide. The sensors were deployed about 20 m north of the centerline of the field, which provided adequate fetch for the BREB method for all wind directions.

Bowen-ratio, weather, and supplementary data were collected at MS002 from DOY 161 to DOY 171. Measured parameters, sensor and data-logger models, scanning intervals, and recording times at MS002 were identical to those at MS001. Deployment heights are listed in Table 4.

5.3. Measurements at MS003

MS003 was located in a winter-wheat field that had been fully grazed, and then overtaken by weeds. Vegetation was dense, and included many species of grasses and

Table 4
Sensor deployment at MS002

Variable	Sensor make and model	Sensor height or depth (m)
Net radiation	REBS Q6	1.32
Deep soil-heat flux	Modified Peltier Coolers (Weaver and Campbell, 1985)	–0.05
Heat-storage flux	Thermocouples	–0.006, –0.019, –0.031, –0.044
Air-temperature difference	Delta-T WVU-7	1.12, 2.12
Vapor-pressure difference	Delta-T WVU-7	1.12, 2.12
Air temperature	Campbell Scientific HMP35C	1.31
Relative humidity	Campbell Scientific HMP35C	1.31
Wind speed	R.M. Young 03001-5	2.24
Wind direction	R.M. Young 03001-5	2.24
Solar radiation	Licor LI-200S	1.41
Photosynthetically active radiation	Licor LI-190S	1.41

forbs (see Table 2) with a mean canopy height of 0.3 m. A farmyard was located about 90 m to the north and a north-south dirt road about 50 m east, possibly interfering with the fetch in those directions, but fetch in all other directions was adequate.

Bowen ratio, weather, and supplementary data were collected at MS003 from DOY 162 to DOY 171. Sensors and deployment heights are listed in Table 5. Air-temperature and vapor-pressure differences were measured using a psychrometer exchange mechanism designed by REBS, after Fritschen and Simpson (1989). Equilibration times, scanning intervals, and recording times for the psychrometers were identical to those at MS001 and MS002. Collection of psychrometric data was interrupted frequently from DOY 162 to DOY 164 because of instrument malfunction; performance improved after DOY 164. Net radiation, weather, and supplementary data collection at MS003 was identical to that at MS001 and MS002.

Table 5
Sensor Deployment at MS003

Variable	Sensor make and model	Sensor height or depth (m)
Net radiation	REBS Q6	1.47
Deep soil-heat flux	Modified Peltier Coolers (Weaver and Campbell, 1985)	–0.05
Heat-storage flux	Thermocouples	–0.006, –0.019, –0.031, –0.044
Air-temperature difference	REBS (Fritschen and Simpson, 1989)	1.02, 2.02
Vapor-pressure difference	REBS (Fritschen and Simpson, 1989)	1.02, 2.02
Air temperature	Campbell Scientific HMP35C	1.26
Relative humidity	Campbell Scientific HMP35C	1.26
Wind speed	R.M. Young 03001-5	1.72
Wind direction	R.M. Young 03001-5	1.72
Solar radiation	Licor LI-200S	1.50
Photosynthetically active radiation	Licor LI-190S	1.50

Table 6
Sensor deployment at MS004

Variable	Sensor make and model	Sensor height or depth (m)
Net radiation	REBS Q6	2.3
Deep soil-heat flux	REBS HFT-3	– 0.05
Heat-storage flux	REBS STP-1	0 to – 0.05
Air-temperature difference	Modified Vaisala HMP35A	0.93, 1.83
Vapor-pressure difference	Modified Vaisala HMP35A	0.83, 1.83
Air temperature	Modified Vaisala HMP35A	0.83, 1.83
Relative humidity	Modified Vaisala HMP35A	0.83, 1.83
Wind speed	Met One 010B	3.0
Wind direction	Met One 5470	3.0
Atmospheric pressure	Met One 090C	1.21
Soil moisture	Soiltest MC300	– 0.02 to – 0.05

5.4. Measurements at MS004

MS004 was located near the southeast corner of a densely vegetated grassy pasture/rangeland composed primarily of weeping lovegrass (*Eragrostis barrelieri* Daveau.) with a mean canopy height of about 0.5 m. Sensors were about 50 m to 60 m north and west of a gravel east-west road lined with trees and 50 to 60 m west of a north-south paved road lined with trees, possibly interfering with the fetch in those directions, but adequate fetch existed in all other directions.

A REBS surface energy balance system (SEBS) was used at MS004 to measure energy flux, weather and supplementary data. The SEBS is an integrated system of sensors designed for the US Department of Energy's Atmospheric Radiation Measurements (ARM) program. Bowen-ratio, weather, and supplementary data were collected beginning on DOY 163. Sensors and deployment heights and depths are listed in Table 6.

R_n was measured using a REBS Q6 net radiometer. Five REBS HFT-3 soil-heat-flux plates were buried at 5 cm to measure G_d , and five platinum resistance thermometer probes were buried to measure the change in soil temperature. Each probe measured the mean temperature between the surface and the 5-cm depth.

Air temperature and vapor pressure differences were measured with modified Vaisala HMP35A temperature-humidity probes. The exchange mechanism, designed by REBS, exchanged sensor positions every 15 min, allowing 2 min for equilibration after each exchange. Measurements from two 15-min periods were averaged to produce a 30-min Bowen ratio.

Wind speed and direction were measured using a Met One 010B anemometer and 5470 wind vane, respectively. Atmospheric pressure was measured using a Met One 090C barometric pressure sensor. Soil moisture was measured over the 2 to 5 cm depth interval, using five Soiltest MC300 soil moisture sensors. This value of soil moisture was used with an estimate of bulk density to compute C in Eq. (6). All sensors on the REBS installation were scanned every 30 s, and 30-min means were recorded on a Campbell Scientific CR10 data logger.

6. Data analysis

6.1. General hydrometeorological conditions

Before the data collection began on June 10 (DOY 162), there were significant rainfall amounts measured by the raingage network (42 continuous recording raingages, see Allen and Naney, 1991) for the period June 5 (DOY 157) to June 9 (DOY 161), with cumulative amounts of over 50 mm recorded by most of the raingages (Schiebe et al., 1993). This was followed by a dry period with no precipitation recorded by the raingage network during the field campaign (see Fig. 3 from Jackson et al., 1995).

A plot of near-surface soil moisture (0–5 cm) estimated from daily gravimetric samples collected near the flux sites is given in Fig. 2. Note that each site shows a general drying trend from DOY 162–170, with slight increases appearing occasionally due to the inherent spatial variation in surface soil moisture. The magnitude of the 0–5 cm soil moisture and rate of drying at the different sites is probably related to the soil texture, and amount of vegetation cover shading the soil surface (Jackson et al., 1993b, 1995). The temporal trace of soil moisture at depths of approximately 25, 40, 55 and 120 cm using the RFC technique indicated little change in the water content during the experimental period with moisture increasing with depth and ranging between 20 and 25% (Heathman, 1993). The moisture profile observations together with the rainfall amounts just prior to the field campaign suggests that there was adequate water available to the vegetation for meeting atmospheric demand.

The daytime average air temperature, wind speed and direction (computed for the period 08:00–19:00 Central Daylight Savings Time (CDST)) are summarized in Fig. 3. This time period was about two hours after sunrise and two hours before sunset with the half-hourly values of $R_n > 100 \text{ W m}^{-2}$ and positive turbulent fluxes. Solar noon

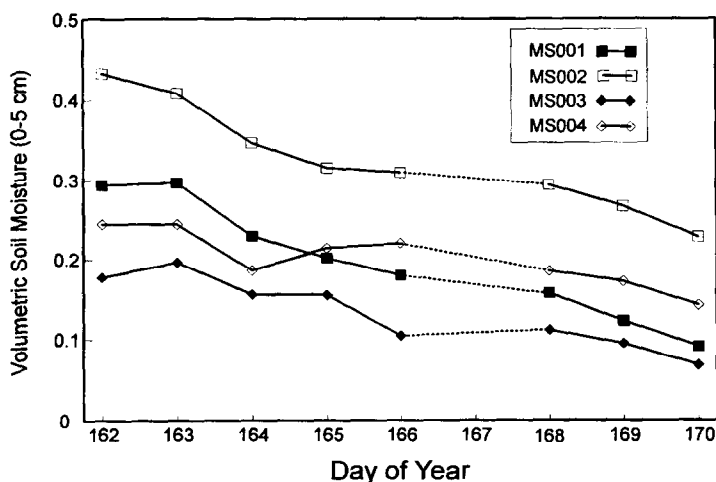


Fig. 2. Plot of near-surface (0–5 cm) volumetric soil moisture estimated from daily gravimetric samples collected near the flux stations.

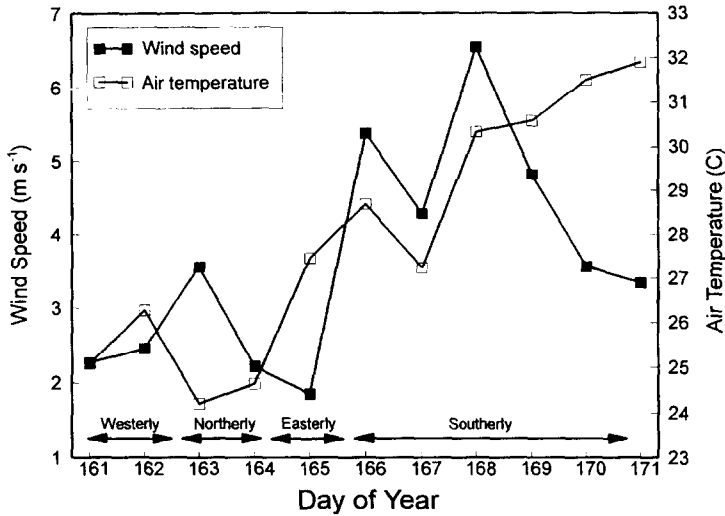


Fig. 3. Daytime (i.e., average of the half-hourly measurements between 08:00–19:00 CDST) air temperature and wind speed from the mean of the measurements collected at the flux stations in operation during the field experiment. Daytime near-surface wind direction is indicated along the abscissa.

occurred around 1330 CDST. Since the trends were similar for all four sites, the average of the four is shown in the figure. There were several significant changes in near surface meteorological conditions from the first to the second half of the field campaign. This included a noticeable shift in surface wind direction from westerly clockwise to easterly during the first half of the field campaign, to southerly during the second half. In addition the second half of the experiment was generally warmer and had greater wind speeds. In Fig. 4, a plot of daytime average air temperature and vapor pressure deficit (VPD) shows that after winds shifted to a southerly direction, there was generally an increase in both temperature and vapor pressure deficit. This indicates an increase in the atmospheric evaporative demand. The anomalous drop in air temperature and VPD on Day 167 was caused by overcast sky conditions (see Fig. 5).

Measurements of incoming solar radiation, R_s , were made at three of the four sites (MS001, MS002 and MS003). The daytime average solar radiation for the three sites is plotted in Fig. 5 for the experimental period when all three sites were collecting daily data. To remove bias in the sensor calibrations, an intercomparison was performed in the field on DOY 170 for a period before local noon when there were uniformly clear skies. Using the average of the three measurements as the standard, the values of R_s computed using the original factory calibrations were adjusted by multiplying the field values by 1.039, 0.981 and 1.0 for MS001, MS002 and MS003, respectively. The comparison in Fig. 5 suggests that on a daily basis, incoming radiation can vary up to 50 W m^{-2} or around 10% over a moderately sized basin. Most days were partly cloudy, with DOY 167 being essentially overcast.

The variation in the daytime average λE and R_n for the 4 sites is illustrated in Fig. 6. For any site, the day to day variability in λE is strongly affected by the amount of

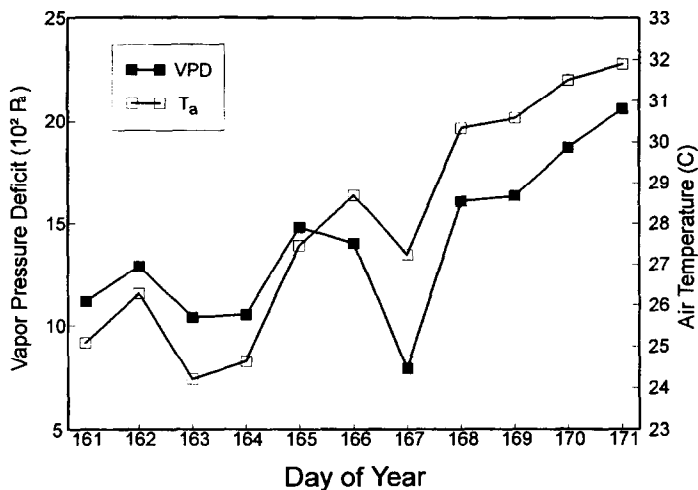


Fig. 4. The mean daytime air temperature and vapor pressure deficit from the flux stations in operation over the experimental period.

radiation. As a result, on a daytime average basis the temporal trends in R_n are similar for all sites leading to a similar time trace in λE . Differences in the magnitude of λE between MS001, MS002, and MS004 are less than 100 W m^{-2} , while MS003 is generally 100 W m^{-2} larger in magnitude, except for the overcast day (DOY 167). With the uncertainty in λE of 10 to 20% and daytime values on the order of $200\text{--}300 \text{ W m}^{-2}$, differences between MS002, MS004 and MS001 are relatively minor, except

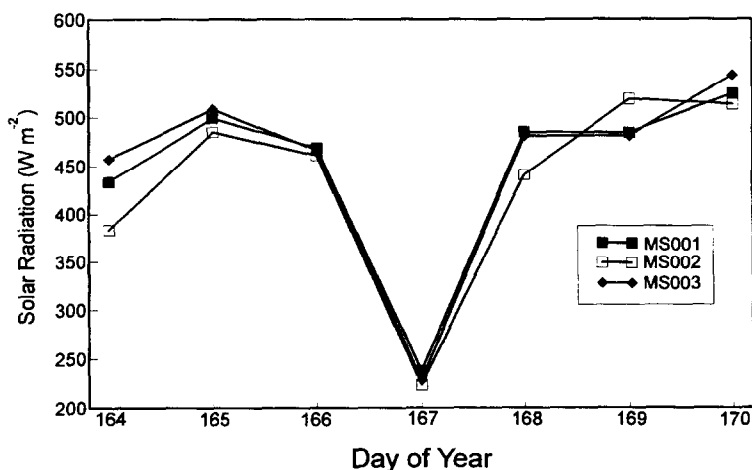


Fig. 5. Daytime solar radiation for MS001, MS002 and MS003 for the period when all three were in operation collecting daily data.

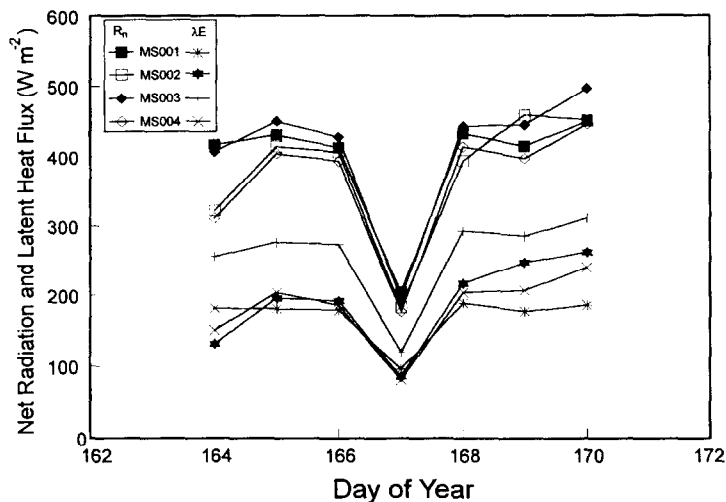


Fig. 6. Daytime average net radiation (R_n) and latent heat flux (λE) for MS001–MS004 over the experimental period DOY 164–170.

possibly for DOY 170. There is, however, a noticeable trend of daytime λE -values from MS002 and MS004 moving closer to the values given by MS003.

But to evaluate relative differences in energy partitioning, and remove some of the scatter in comparing λE -values caused by variation in R_n between sites, requires the use of parameters such as the evaporative fraction, EF. Comparisons among the sites using EF are now discussed.

6.2. Comparison of energy partitioning at the four flux sites

Compared to Fig. 6, the gradual increase in the amount of available energy being converted to λE for MS002 and MS004 is more evident when the daytime average evaporative fraction, EF, are plotted (Fig. 7) for the period with significant increase in air temperature and vapor pressure deficit (DOY 164–170). The values of EF were calculated by summing the half-hourly fluxes of H and λE over the period 08:00–19:00 CDST.

From Fig. 7, there appears to be significant differences in the magnitude and temporal trend of EF for some of the sites. For MS003, the EF-values in Fig. 7 indicate a fairly uniform trend varying between 0.7 and 0.75. Similarly for MS001 EF stays relatively constant between 0.6 and 0.65, except for DOY 167, the overcast day. A possible explanation for the greater increase in EF at MS001 on DOY 167 than at the other sites is that there was a significant reduction in sensible heat flux from the bare soil due to the low radiation load that day for heating the bare ground surface. Since MS001 had only a 50% cover, the stomatal response to the significant reduction in radiation by the vegetation (Jarvis, 1976), which would tend to conserve EF at the other sites having nearly complete cover, would not have the same impact on EF for this site.

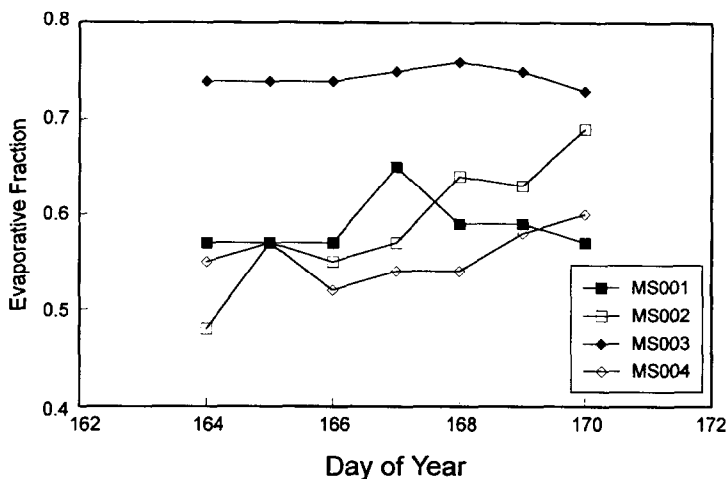


Fig. 7. Daytime average values of evaporative fraction (EF) for MS001–MS004 covering DOY 164–170.

The temporal behavior in EF for MS002 and MS004 differ markedly from the other two. Both start lower on DOY 164 and gradually increase, especially MS002. This trend in EF seems to be related to the temporal trend in VPD (see Fig. 4), which shows a general increase (except for DOY 167) over the experimental period. The influence of VPD on EF for MS002 and MS004 is illustrated in a plot of EF versus the daytime average VPD in Fig. 8. The general trend of increasing EF with higher VPD, given by the least squares regression line using the data from both sites (but excluding the data for DOY 167; see Fig. 8), has a correlation of 0.67. The relationship between EF and

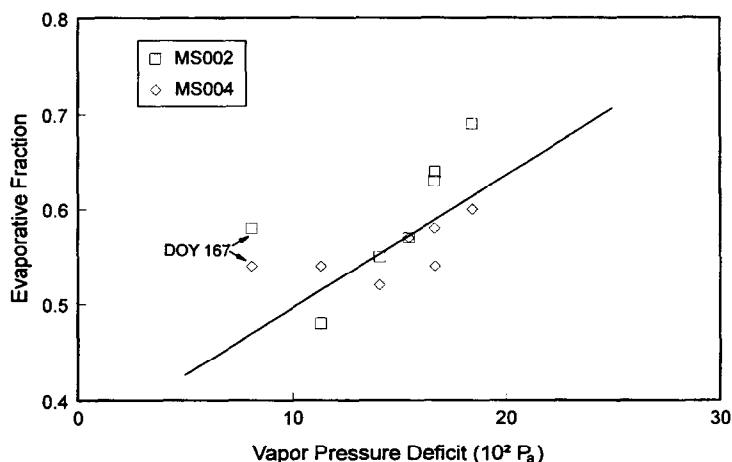


Fig. 8. Comparison of daytime average values of evaporative fraction (EF) versus vapor pressure deficit (VPD) for MS002 and MS004. The line represents the least squares regression equation using the data from both sites, except for DOY 167 the overcast day. The data points from DOY 167 are labeled in the figure.

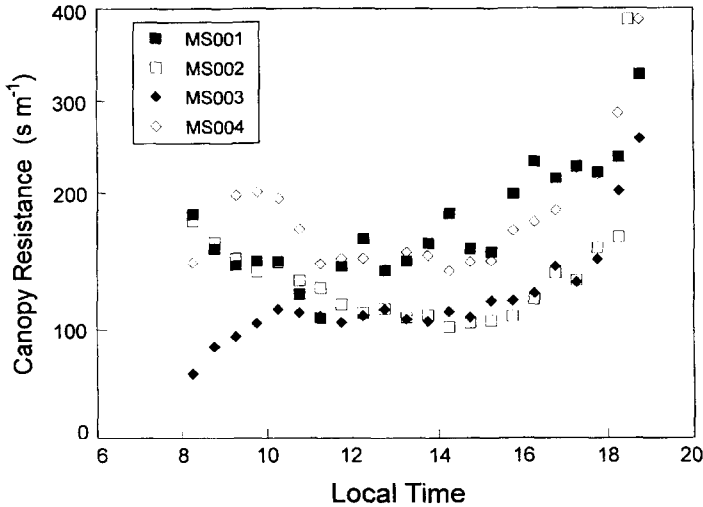


Fig. 9. Half-hourly values of the canopy resistance (r_c) for MS001–MS004 for DOY 170.

VPD is similar to the observations from Verma et al. (1986) over a deciduous forest (see also Baldocchi, 1989). This result suggests that the grasses at MS002 and MS004 were more closely coupled to the atmosphere than the weeds at MS001 and MS003, since the latter did not have a similar response to VPD. Further evidence showing a varying response from the vegetation at the four sites to the atmospheric forcing was obtained by computing midday values of r_c and r_s described in the next section.

6.3. Comparison of Penman–Monteith and Priestley–Taylor parameters

The temporal trend in r_c was investigated using Eq. (1). Values of r_c were first computed using the half-hourly data as suggested by Stewart (1989). These were then averaged over the period 1200 to 1700 CDST and defined as ‘midday’ values. It was observed, as in other studies (e.g. Kim and Verma, 1991), that there is a time period where r_c -values are relatively constant (see Fig. 9). Sensitivity to the averaging period was evaluated by computing midday values of r_c over a shorter period (i.e. 1200–1400 CDST). The result was only a minor change (i.e. less than 10% on average) in midday r_c from the values computed using the former averaging period. The same averaging period was used to compute ‘midday’ values of α from Eq. (3).

To compute r_{av} with Eq. (2), estimates of the roughness parameters, d_o and z_{om} were required. The local roughness length, z_o , and displacement, d_o , for MS002, MS003 and MS004 were estimated by taking $\frac{1}{10}$ and $\frac{2}{3}$ of the average canopy height, respectively (Brutsaert, 1982). Modeling and observational studies indicate that the ratio of z_o to obstacle height, h , (z_o/h) varies with the density of the roughness elements (Brutsaert, 1982). With a 50% canopy cover for MS001, d_o was assumed to equal half the average canopy height, and by using the relationship $z_o/h = 0.29(1 - d_o/h)$ from Shaw and Pereira (1982), this indicated z_o was about $\frac{1}{7}$ the vegetation height.

Since MS001 had around 50% vegetation cover, the Penman–Monteith approach for estimating r_c is not appropriate (Stannard, 1993). Unfortunately, there was not sufficient information for using a more physically-based two-component model such as Shuttleworth and Wallace (1985) for evaluating the contribution of evaporation from the soil and vegetation. However, a simplified approach described by Kustas (1990) for estimating the energy balance of the soil surface was used in order to determine the soil contribution to evaporation. The approach estimates R_n at the soil surface using the Beer's Law exponential decay relation with the estimate of LAI (see Table 2). With measurements of G , λE from the soil was determined by Eq. (7) with the Bowen ratio of the soil surface estimated from results of simulations of a drying soil with a four-layer heat budget model by Choudhury and Monteith (1988). Starting on DOY 164, a couple of days after saturated soil conditions, the value of β for the soil increased from 1 to 3 on DOY 165 to 4 on DOY 166 to an upper limit of 6 for the remaining four days (see Fig. 3 from Choudhury and Monteith, 1988). Thus λE from the vegetation (λE_{veg}) was computed as the difference between the λE from the soil and λE from the BREB system. Radiometric measurements of the canopy temperatures at MS001 collected over the course of several days indicated that vegetation-air temperature differences were negligible. Hence the value of r_c was computed by the following expression:

$$r_c = \rho c_p \frac{e_a^* - e_a}{\gamma \lambda E_{veg}} - r_{av} \quad (9)$$

Although estimating r_c with Eq. (9) is somewhat tenuous, compared to using Eq. (1) it should provide values of r_c that are less influenced by changes in the soil surface evaporation.

The midday values of r_c for the period DOY 164–170 are shown in Fig. 10. Notice in the figure the fairly pronounced decrease in r_c for MS002, and to a lesser degree for MS004, going from DOY 164 to 170. There is no consistent temporal trend in r_c for

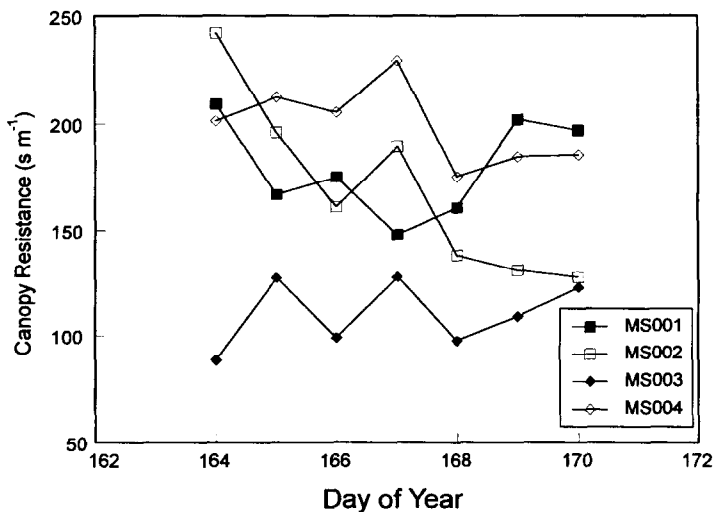


Fig. 10. Midday values of the canopy resistance (r_c) for MS001–MS004 during the period DOY 164–170.

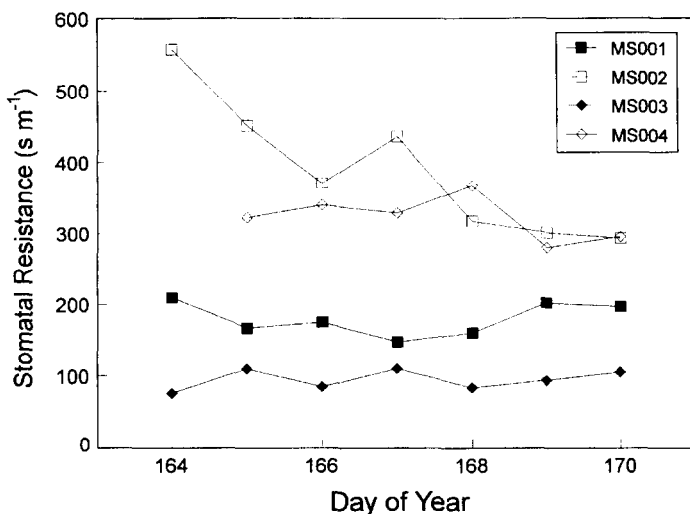


Fig. 11. Midday representative values of the stomatal resistance (r_s) for MS001–MS004 covering DOY 164–170.

MS001 and MS003. In addition, note that r_c increases for MS002, MS003 and MS004 for the overcast day (DOY 167) as expected from the relationship between stomatal response to radiation (Jarvis, 1976), but decreases for MS001. This result for MS001 is probably not real and indicates deficiencies in the approach summarized by Eq. (9) for estimating r_c . The range in r_c under well-watered conditions is similar, but somewhat larger to observations of a temperate grassland ecosystem (Kim and Verma, 1990; Kim and Verma, 1991; Stewart and Verma, 1992), where during the early growth stages the unstressed values of midday r_c were typically on the order of 50–100 s m^{-1} and during the early stage of senescence where midday values of r_c were on the order of 100–150 s m^{-1} .

Stronger differences between and similarities among sites were apparent when midday values of r_s were calculated with Eq. (3). The results are illustrated in Fig. 11. For MS002 and MS004 (the pasture/rangeland sites with predominately grasses) the r_s -values are similar and range mainly between 300 and 400 s m^{-1} . The sites with weedy vegetation have r_s -values between 150 and 200 s m^{-1} for MS001 and between 80 and 100 s m^{-1} for MS003. This indicates that plant physiological differences between the grasses and weeds is probably the main reason for differences in vegetation water use and energy partitioning for MS002 and MS004 versus MS001 and MS003. Estimates of r_s using Eq. (3) with observations from Kim and Verma (1991), where LAI was on the order of 2 during early growth and senescent stages (see their Fig. 1), yields a range in r_s from 100 to 300 s m^{-1} . Thus the r_s -values for most sites fall close to or inside this range, suggesting that the estimates r_c and r_s with the present data are reasonable.

The midday values of α were computed with Eq. (4) for the same period, DOY 164–170. The values of α for all sites were between 0.6 and 1 (see Fig. 11), even

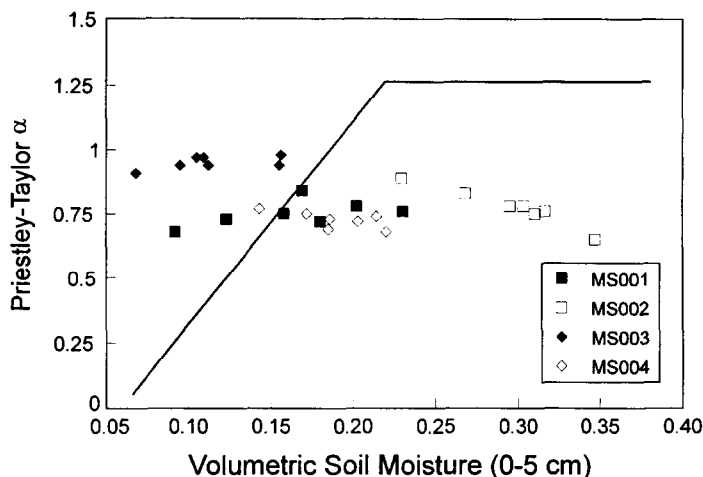


Fig. 12. Midday values of the Priestley–Taylor parameter α for MS001–MS004 versus the near-surface (0–5 cm) volumetric soil moisture estimates from Fig. 2 for the period DOY 164–170. The curve is Eq. (2) from Crago and Brutsaert (1992).

though the plants were well supplied with water and the near-surface soil moisture remained relatively high until near the end of the study period (Fig. 2). However, the magnitudes of the canopy resistance estimated for these sites were usually between 100 and 200 s m^{-1} , which forces α to be less than one (de Bruin, 1983; McNaughton and Spriggs, 1989).

In Fig. 12, the α -values for each site are compared to the near-surface soil moisture measurements from Fig. 2. Also displayed is Eq. (2) from Crago and Brutsaert (1992), which was fit to the FIFE data. In general, there appears to be no trend in α with near-surface soil moisture as found in previous studies (e.g. Barton, 1979; Davies and Allen, 1973; Crago and Brutsaert, 1992). This result suggests that changes in near-surface soil moisture had little effect on energy partitioning at these sites and is, at least in part, caused by the fact that there was no significant relationship between changes in near-surface soil moisture and changes in the root zone water content (i.e. at depths of 10 to 50 cm). Although studies have shown that there is a correlation between profile and surface soil moisture, the relationship depends on many factors including hydrological properties of the soils and vegetation type and cover (Kostov and Jackson, 1993). For example, soil texture and porosity are important factors to consider because a relationship between near-surface soil moisture and α will be different for well drained versus poorly drained soils (e.g. Davies and Allen, 1973). The soils at MS001 and MS002 are similar to the soils in FIFE, but only the points from MS001 fall around the curve. In general, one should follow the recommendation of Davies and Allen (1973) who suggest that you should only use surface soil moisture in estimating α for bare soil and shallowly rooted vegetated surfaces.

Unfortunately, data were not collected under a full range of near-surface soil moisture conditions for all the sites. Without a full range in conditions, we cannot determine if α

rapidly decreases below a certain near-surface soil moisture threshold (e.g. Crago and Brutsaert, 1992). Therefore, no definitive conclusions can be made about the behavior of α with near-surface soil moisture at the drier end.

7. Concluding remarks

The partitioning of available energy from 4 sites during Washita '92 were analyzed using the BREB method. The change in daytime average EF observed over the experimental period suggested that an increasing atmospheric demand tended to have a larger effect on the partitioning of available energy than did drying of the soil, although this was only evident for the pasture/rangeland sites (MS002 and MS004) and not for sites containing weedy vegetation (MS001 and MS003).

Values of canopy resistance r_c from the Penman–Monteith equation, and estimates of effective stomatal resistance r_s using Eq. (3) provided additional insight into the impact on vegetation water use at the four sites due to changes in atmospheric demand. Clearly, not all sites contained vegetation that responded similarly to atmospheric demand. The values of r_s indicated that the grassy vegetation at pasture/rangeland sites had similar physiological characteristics which were different from the sites containing weedy vegetation. For all sites, α was below 1, suggesting a significant canopy resistance (de Bruin, 1983). Furthermore, relationships between α and surface soil moisture found for short vegetation (e.g. Davies and Allen, 1973; Crago and Brutsaert, 1992) were not observed at these sites. However, observations over a wider range of surface soil moisture conditions is required to know the generality of these results.

The present study indicates that within mixed agricultural- rangeland environments, there can be considerable spatial and temporal variation in EF. This resulted in the variation of key parameters in two commonly used evaporation models, the Penman–Monteith and Priestley–Taylor approaches. For the Penman–Monteith model, the typical range in r_c was from 100 to 200 s m⁻¹ while for the Priestley–Taylor model, α varied between 1 and 0.6. The variability in response of the vegetation at the various sites to atmospheric forcing suggests that defining characteristic values of r_c for broad land use classes, such as done in mesoscale atmospheric models, may not always be appropriate (Pielke and Avissar, 1990). The variation in EF, which indicates the relative partitioning of the available energy into latent and sensible heat fluxes, and how it may impact atmospheric circulations when these areas have significant spatial extent have been simulated in atmospheric models (Segal and Arritt, 1992). However, observations of surface flux variability for validating model results in different climatic regions are generally lacking. Therefore, to gain more confidence in model simulations, longer term data, than what was collected in this study, indicating the typical magnitudes of the spatial and temporal variations in EF for the main land use classes in mixed agricultural-rangeland environments are desperately needed.

Acknowledgements

The authors would like to thank Drs. Frank R. Schiebe and Thomas J. Jackson of USDA–ARS and Dr. Edwin T. Engman of NASA for their cooperation and assistance in

making this experiment possible. In addition, we would like to thank the personnel at the USDA–ARS Little Washita River Watershed Field Office in Chickasha for handling much of the logistics during the field campaign. The authors would like to acknowledge the assistance and guidance of Dr. Robert D. Williams, Plant Physiologist at the USDA–ARS National Agricultural Water Quality Laboratory, who provided the vegetation data and information on plant species for this paper.

References

- Allen, P.B. and Naney, J.W., 1991. Hydrology of the Little Washita River Watershed, Oklahoma: Data and analyses, Tech. Rep. ARS-90. US Department of Agriculture, Agric. Research Service, Durant, OK, 74 pp.
- Avisar, R., 1993. Observations of leaf stomatal conductance at the canopy scale: an atmospheric modeling perspective. *Boundary-Layer Meteorol.*, 64: 127–148.
- Baldocchi, D., 1989. Canopy–atmosphere water vapor exchange: Can we scale from a leaf to a canopy? In: *Proceedings of Estimation of Areal Evapotranspiration*. IAHS Publ. No. 177. pp. 21–41.
- Baldocchi, D.D., Luxmore, R.J. and Hatfield, J.L., 1991. Discerning the forest from the trees: An essay on scaling canopy stomatal conductance. *Agric. For. Meteorol.*, 54: 197–226.
- Barton, I.J., 1979. A parameterization of the evaporation from nonsaturated surfaces. *J. Appl. Meteorol.*, 18: 43–47.
- Beljaars, A.C.M., Viterbo, P.M., Miller, J., Betts, A.K. and Ball, J.H., 1993. A new surface boundary layer formulation at ECMWF and experimental continental precipitation forecasts (July 1993). *GEWEX News*, 3(3): 1–9.
- Bell, J.P., Dean, T.J. and Hodnett, M.G., 1987. Soil moisture measurements by an improved capacitance technique. Part II: Field techniques, evaluation and calibration. *J. Hydrol.*, 93: 79–90.
- Bowen, I.S., 1926. The ratio of heat losses by conduction and evaporation from any water surface. *Phys. Rev.*, 27: 779–787.
- Brutsaert, W., 1982. *Evaporation into the Atmosphere*. D. Reidel, Dordrecht, 299 pp.
- Choudhury, B.J., Ahmed, N.U., Idso, S.B., Reginato, R.J. and Daughtry, C.S.T., 1994. Relations between evaporation coefficients and vegetation indices studied by model simulations. *Remote Sens. Environ.*, 50: 1–17.
- Choudhury, B.J. and Monteith, J.L., 1988. A four-layer model for the heat budget of homogeneous land surfaces. *Q. J. R. Meteorol. Soc.*, 114: 373–398.
- Crago, R.D. and Brutsaert, W., 1992. A comparison of several evaporation equations. *Water Resour. Res.*, 28: 951–954.
- Davies, J.A. and Allen, C.D., 1973. Equilibrium, potential and actual evaporation from cropped surfaces in southern Ontario. *J. Appl. Meteorol.*, 12: 649–657.
- de Bruin, H.A.R., 1983. A model for the Priestley–Taylor parameter α . *J. Clim. Appl. Meteorol.*, 22: 572–578.
- Dean, T.J., Bell, J.P. and Baty, A.J., 1987. Soil moisture measurements by an improved capacitance technique. Part I: Sensor design and performance. *J. Hydrol.*, 93: 67–78.
- Finnigan, J.J. and Raupach, M.R., 1987. Modern theory of transfer in plant canopies in relation to stomatal characteristics. In: E. Zeiger, G. Farquhar and I. Cowen (Editors), *Stomatal Function*. Stanford University Press, Stanford, CA, pp. 385–429.
- Flint, A.L. and Childs, S.W., 1991. Use of Priestley–Taylor evaporation equation for soil water limited conditions in a small forest clearcut. *Agric. For. Meteorol.*, 56: 247–260.
- Fritschen, I.J. and Simpson, J.R., 1989. Surface energy and radiation balance systems: general description and improvements. *J. Appl. Meteorol.*, 28(7): 680–689.
- Heathman, G. C., 1993. Chapter XIV. Profile Soil Moisture. In: T.J. Jackson and F.R. Schiebe (Editors), *Hydrology Data Report Washita '92, NAWQL 93-1*. National Agricultural Water Quality Laboratory, US Department of Agriculture, Agricultural Research Service, Durant, OK, 6 pp.

- Heilman, J.L., Brittin, C.L. and Neale, C.M.U., 1989. Fetch requirements for Bowen ratio measurements of latent and sensible heat fluxes. *Agric. For. Meteorol.*, 44: 261–273.
- Jackson, T.J., Engman, E.T. and Schiebe, F.R., 1993a. Chapter I. Washita '92 Experiment Description. In: T.J. Jackson and F.R. Schiebe (Editors), *Hydrology Data Report Washita '92*, NAWQL 93-1. National Agricultural Water Quality Laboratory, US Department of Agriculture, Agricultural Research Service, Durant, OK, 2 pp.
- Jackson, T.J., Le Vine, D.M., Schiebe, F.R. and Schmugge, T.J., 1993b. Large area mapping of soil moisture using passive microwave radiometry in the Washita '92 experiment. *Proc. Inter. Geosci. Remote Sens. Symp. (IGARSS '93) Better Understanding of Earth Environment*, Kogakuin University, Tokyo, Japan, August 18–21, Vol. III, pp. 1009–1012.
- Jackson, T.J., Le Vine, D.M., Swift, C.T., Schmugge, T.J. and Schiebe, F.R., 1995. Large area mapping of soil moisture using the ESTAR passive microwave radiometer in Washita '92. *Remote Sens. Environ.*, 53: 27–37.
- Jackson, T.J., Ridgway, T. and Filho, O., 1993c. Chapter X. Soil bulk density sampling. In: T.J. Jackson and F.R. Schiebe (Editors), *Hydrology Data Report Washita '92*, NAWQL 93-1. National Agricultural Water Quality Laboratory, US Department of Agriculture, Agricultural Research Service, Durant, OK, 2 pp.
- Jarvis, P.G., 1976. The interpretation of the variations in leaf water potential and stomatal conductance found in canopies in the field. *Philos. Trans. R. Soc. London, Ser. B*, 273: 593–610.
- Jarvis, P.G. and McNaughton, K.G., 1986. Stomatal control of transpiration: scaling up from leaf to region. *Adv. Ecol. Res.*, 15: 1–45.
- Kim, J. and Verma, S.B., 1990. Components of surface energy balance in a temperate grassland ecosystem. *Boundary-Layer Meteorol.*, 51: 401–417.
- Kim, J. and Verma, S.B., 1991. Modeling canopy stomatal conductance in a temperate grassland ecosystem. *Agric. For. Meteorol.*, 55: 149–166.
- Kostov, K.G. and Jackson, T.J., 1993. Estimating profile soil moisture from surface layer measurements—a review. *Proc. Soc. Photo-Opt. Instrum. Engin. Ground Sens.*, 1941: 125–136.
- Kustas, W.P., 1990. Estimates of evapotranspiration with a one- and two-layer model of heat transfer over partial canopy cover. *J. Appl. Meteorol.*, 29: 704–715.
- McNaughton, K.G. and Jarvis, P.G., 1991. Effects of spatial scale on stomatal control of transpiration. *Agric. For. Meteorol.*, 54: 279–301.
- McNaughton, K.G., and Spriggs, T.W., 1989. An evaluation of Priestley and Taylor equation and the complementary relationship using results from a mixed-layer model of the convective boundary layer. In: *Proceedings of Estimation of Areal Evapotranspiration*. IAHS Publ. No. 177, pp. 89–104.
- Monteith, J.L., 1973. *Principles of Environmental Physics*. Edward Arnold, London, 241 pp.
- Nie, D., Kanemasu, E.T., Fritschen, L.J., Weaver, H.L., Smith, E.A., Verma, S.B., Field, R.T., Kustas, W.P. and Stewart, J.B., 1992. An intercomparison of surface energy flux measurement systems used during FIFE 1987. *J. Geophys. Res.*, 97(D17): 18715–18724.
- Pielke, R.A. and Avissar, R., 1990. Influence of landscape structure on local and regional climate. *Landscape Ecol.*, 4: 133–155.
- Priestley, C.H.B. and Taylor, R.J., 1972. On the assessment of surface heat flux and evaporation using large-scale parameters. *Monthly Weather Rev.*, 100: 81–92.
- Segal, M. and Arritt, R.W., 1992. Nonclassical mesoscale circulations caused by surface sensible heat-flux gradients. *Bull. Am. Meteorol. Soc.*, 73: 1593–1604.
- Schiebe, F.R., Hicks, A.D. and Jackson, T.J., 1993. Chapter III. Hydrology. In: T.J. Jackson and F.R. Schiebe (Editors), *Hydrology Data Report Washita '92*, NAWQL 93-1. National Agricultural Water Quality Laboratory, US Department of Agriculture, Agricultural Research Service, Durant, OK, 8 pp.
- Shaw, R.H. and Pereira, A.R., 1982. Aerodynamic roughness of a plant canopy: a numerical experiment. *Agric. Meteorol.*, 29: 51–65.
- Shuttleworth, W.J., 1976. A one-dimensional theoretical description of the vegetation–atmosphere interaction. *Boundary-Layer Meteorol.*, 10: 273–302.
- Shuttleworth, W.J. and Wallace, J.S., 1985. Evaporation from sparse crops—An energy combination theory. *Q. J. R. Meteorol. Soc.*, 111: 839–855.
- Sinclair, T.R., Allen Jr., L.H. and Lemon, E.R., 1975. An analysis of errors in the calculation of energy flux densities above vegetation by a Bowen-ratio profile method. *Boundary-Layer Meteorol.*, 8: 129–139.

- Stannard, D.I., 1985. Design and performance of a machine used in the calculation of Bowen ratios: National Water Well Association, Proceedings of the Conference on Characterization and Monitoring of the Vadose (Unsaturated) Zone, Denver, 1985. pp. 143–157.
- Stannard, D.I., 1993. Comparison of Penman–Monteith, Shuttleworth–Wallace and modified Priestley–Taylor evapotranspiration models for wildland vegetation in semiarid rangeland. *Water Resour. Res.*, 29: 1379–1392.
- Stannard, D.I., Kustas, W.P., Allwine, K.J. and Anderson, D.E., 1993. Chapter V. Micrometeorological data collection. In T.J. Jackson and F.R. Schiebe (Editors), *Hydrology Data Report Washita '92, NAWQL 93-1*. National Agricultural Water Quality Laboratory, US Department of Agriculture, Agricultural Research Service, Durant, OK, 17 pp.
- Stewart, J.B., 1989. On the use of the Penman–Monteith equation for determining areal evapotranspiration. In: *Proceedings of Estimation of Areal Evapotranspiration*. IAHS Publ. No. 177, pp. 3–12.
- Stewart, J.B. and Verma, S.B., 1992. Comparison of surface fluxes and conductances at two contrasting sites within the FIFE area. *J. Geophys. Res.*, 97(D17): 18623–18628.
- Tanner, C.B., 1960. Energy balance approach to evapotranspiration from crops. *Soil Sci. Soc. Am. Proc.*, 24: 1–9.
- Verma, S.B., Baldocchi, D.D., Anderson, D.E., Matt, D.R. and Clement, R.J., 1986. Eddy fluxes of CO₂, water vapor and sensible heat over a deciduous forest. *Boundary-Layer Meteorol.*, 36: 71–91.
- Weaver, H.L. and Campbell, G.S., 1985. Use of peltier coolers as soil heat flux transducers. *Soil Sci. Soc. Am. J.*, 49(4): 1065–1067.
- Williams, R.D., 1993. Chapter VIII. Vegetation sampling. In: T.J. Jackson and F.R. Schiebe (Editors), *Hydrology Data Report Washita '92, NAWQL 93-1*. National Agricultural Water Quality Laboratory, US Department of Agriculture, Agricultural Research Service, Durant, OK, 6 pp.